

Acoustic control of suspended particles in micro fluidic chips

Andreas Nilsson,^a Filip Petersson,^a Henrik Jönsson^b and Thomas Laurell^a

^a Department of Electrical Measurements, Lund Institute of Technology, P.O. Box 118, S-222 10 Lund, Sweden

^b Department of Cardiothoracic Surgery, Lund University Hospital, Lund, Sweden

Received 24th October 2003, Accepted 11th December 2003

First published as an Advance Article on the web 9th February 2004

A method to separate suspended particles from their medium in a continuous mode at microchip level is described. The method combines an ultrasonic standing wave field with the extreme laminar flow properties obtained in a silicon micro channel. The channel was 750 μm wide and 250 μm deep with vertical side walls defined by anisotropic wet etching. The suspension comprised "Orgasol 5 μm " polyamide spheres and distilled water. The channel was perfused by applying an under pressure (suction) to the outlets. The channel was ultrasonically actuated from the back side of the chip by a piezoceramic plate. When operating the acoustic separator at the fundamental resonance frequency the acoustic forces were not strong enough to focus the particles into a well defined single band in the centre of the channel. The frequency was therefore changed to about 2 MHz, the first harmonic with two pressure nodes in the standing wave, and consequently two lines of particles were formed which were collected *via* the side outlets. Two different microchip separator designs were investigated with exit channels branching off from the separation channel at angles of 90° and 45° respectively. The 45° separator displayed the most optimal fluid dynamic properties and 90% of the particles were gathered in 2/3 of the original fluid volume.

1 Introduction

Several particle separation techniques utilizing ultrasound have previously been presented.^{1–8} These are based on the fact that suspended particles exposed to an ultrasonic standing wave field are affected by an acoustic radiation force. This force will move the particles towards either the pressure nodes or the pressure anti-nodes depending on the density and compressibility of the particles and the medium. In order to realise these systems conventional precision engineering has been utilized to create well defined flow-through acoustic resonance cavities in which particles can be manipulated under controlled conditions. To obtain good particle aggregation in such cavities the sidewalls reflecting the acoustic wave must have a low surface roughness and the wall spacing must be constant throughout the separation region. The separation method presented herein is based on the same principle but proposes a different orientation of the piezoceramic actuator. Also, most importantly, modern micro fabrication technologies were utilized in order to address the issue of tedious manufacturing using traditional machining techniques to realise the micro fluidic system. The anisotropic wet etching properties of silicon ensure a perfect alignment of the reflecting walls in the channel. As in all micro fabrication the production of such particle separation structures also benefits from batch fabrication. The particle suspension is fed into a separation channel where it is exposed to an acoustic standing wave field induced by a piezoceramic plate glued to the back side of the silicon structure. The ultrasound frequency is tuned to match one half of the wavelength to the channel width. This results in a pressure nodal plane along the middle of the channel and one pressure anti-nodal plane along each channel side wall. If the density and compressibility of the particles are suitable, compared to the medium, they will move towards the nodal plane while travelling along the separation channel. The end of the channel is split into three outlets and when operating the system in the first harmonic resonance mode ($2 \cdot \lambda/2$) the particles are focused in two pressure nodes leaving the separation channel through the side outlets and a particle free clear medium thus exits through the centre outlet.

2 Theory

2.1 Acoustic force

An acoustic standing wave is commonly described according to eqn. (1).

$$y = A \cdot \cos\left(\frac{2\pi x}{\lambda} + \frac{\phi}{2}\right) \cdot \sin\left(\frac{2\pi t}{T} + \frac{\phi}{2}\right) \quad (1)$$

Eqn. (1) expresses the displacement (y) of a point in the standing wave corresponding to a certain position (x) and time (t). The displacement is also dependent of the amplitude of the standing wave (A), the wavelength (λ), the time for one full period (T) and the phase difference between the two travelling waves (ϕ). By looking at the cosine part of the equation it becomes evident that the distance between two consecutive nodes is $\lambda/2$.

If particles in a liquid are subjected to an ultrasonic field they experience pressure fluctuations. These fluctuations arise from the displacement of the molecules of the medium. If the acoustic field is in the form of a standing wave, eqn. (1) can be rewritten in terms of pressure [eqn. (2)].

$$p = p_0 \cdot \sin(kx) \cdot \cos(\omega t) \quad (2)$$

The constants $k = (2\pi/\lambda)$ and $\omega = (2\pi/T)$ have been introduced and the phase difference has been omitted since it only results in a lateral displacement of the wave. Sonic acoustic waves in a liquid are longitudinal which means that the particles are displaced along the wave. This results in compression and decompression of the particles in the medium. At the pressure nodes the molecular displacement is at its maximum and at the pressure anti-nodes at its minimum. The pressure fluctuations result in forces that act laterally on the particles in the x -direction. According to the acoustic force theory presented by Yosioka and Kawasima⁹ the force on a particle can be expressed in the following way [eqn. (3)].

$$F_r = -\left(\frac{\pi p_0^2 V_c \beta_w}{2\lambda}\right) \cdot \phi(\beta, \rho) \cdot \sin(2kx) \quad (3)$$



$$\phi = \frac{5\rho_c - 2\rho_w}{2\rho_c + \rho_w} - \frac{\beta_c}{\beta_w} \quad (4)$$

V_c is the volume of the particle, p_0 is the pressure amplitude from eqn. (2) and ϕ is defined by eqn. (4). The density of the medium and particles are denoted ρ_w and ρ_c respectively and the corresponding compressibilities β_w and β_c .

Small particles can generally be trapped in an acoustic standing wave. The first criterion is that the particle diameter must be less than half the wavelength, otherwise the acoustic force will act in more than one direction on the particle. The second criterion is that ϕ must not equal zero, otherwise there will be no net force exerted on the particle.

3 Materials and methods

3.1 Micro fabrication

In order for the acoustic separator to work, precise channel structures with vertical walls and good reflective properties are required. Silicon fits these requirements very well. By using photolithography and anisotropic wet etching it is simple to produce structures of rectangular cross-section using $\langle 100 \rangle$ silicon. If a cross-type structure with vertical channel walls is desired, the separation channels on the photo mask are turned 45° in relation to the primary flat of the wafer, (design I, Fig. 1). The separation structure will thereby obtain vertical walls in all flow channels. Optionally, the side channels can be anisotropically defined according to design II (Fig. 1). This separation structure will however get a V-groove cross-section of the side channels due to the slanted $\langle 111 \rangle$ -planes that define the stop etch conditions (Fig. 2). For clarity this design is henceforth denoted “ 45° -separation structure”.

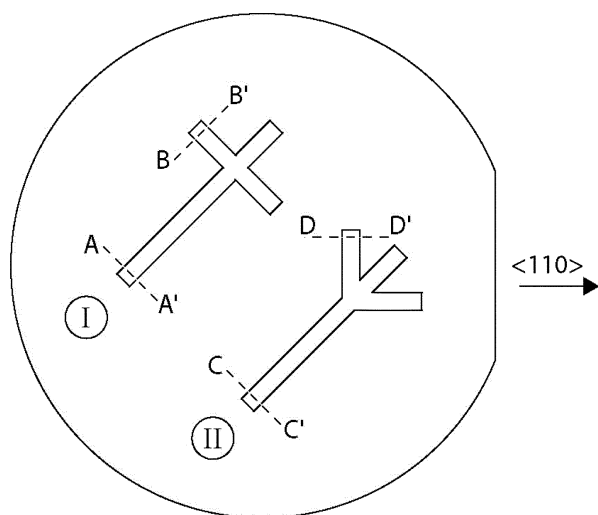


Fig. 1 Separation structures defined on a $\langle 100 \rangle$ silicon wafer. Design I – Cross-type separator; Design II – 45° separation structure.

Double sided photolithography and etching in KOH (potassium hydroxide, Merck KGaA, 64271 Darmstadt, Germany), 40 g in 100 ml deionised water, yielded micro channels with a depth and width of $250 \mu\text{m}$ and $750 \mu\text{m}$ respectively and inlets and outlets etched from the rear side. The micro separator was sealed with a glass lid by means of anodic bonding to achieve a closed separation structure with optical access (Fig. 3).

3.2 Device assembly

The ultrasonic standing waves were generated by PZ26 piezo-electric ceramics (Ferroperm Piezoceramics A/S, Kvistgard, Denmark) with resonance frequencies of 1 MHz and 2 MHz. To achieve an actuation with the highest energy transmission possible, the transducer was glued to the back side of the separation chip with epoxy (2 Ton Clear Epoxy, ITWDevcon, Danvers, MA, USA). The fact that it was glued to the rear side also provided air backing to the transducer, minimizing acoustic losses.

3.3 Experimental arrangement

Silicone rubber tubing was glued to the inlets and outlets on the back side of the separation chip, acting as docking ports to the syringe pump (WPI SP260P, World Precision Instruments, USA) via standard 1/16" od Teflon tubing. The particle suspension used was a Doppler fluid (Dansk Fantom Service, Gondolvej 25, 4040 Jyllinge, Denmark) that consisted of suspended Orgasol particles of $5 \mu\text{m}$ diameter mixed with distilled water. The piezoceramic element was operated via a high frequency power amplifier (Amplifier Research Model 50A15, Amplifier Research, Souderton, PA, USA). The frequency was set by a function generator (HP 3325A, Hewlett-Packard Inc, Palo Alto, CA, USA). After the separation step, particle content of the clear and the enriched fluid was measured by centrifugation using a Haematokrit 2010 (Hettich Zentrifugen, D-78532 Tuttlingen, Germany). Each sample was centrifuged for two minutes at 13000 rpm after which the length of the solid and fluid fraction in the capillaries was measured to determine the percentage solid in each collected volume, A and B. The separation efficiency was subsequently determined as the ratio of the percentage solid fraction in the side outlets from the chip (B)

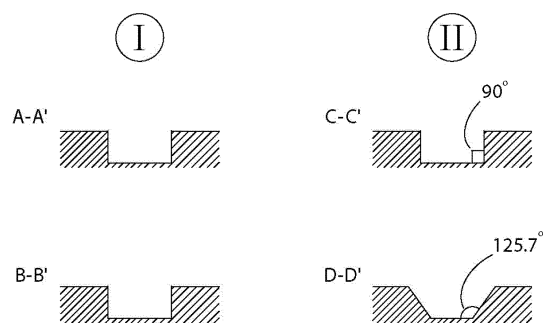


Fig. 2 Cross-sections of the two different designs: I) The cross-type separation structure and II) the 45° -separation structure.

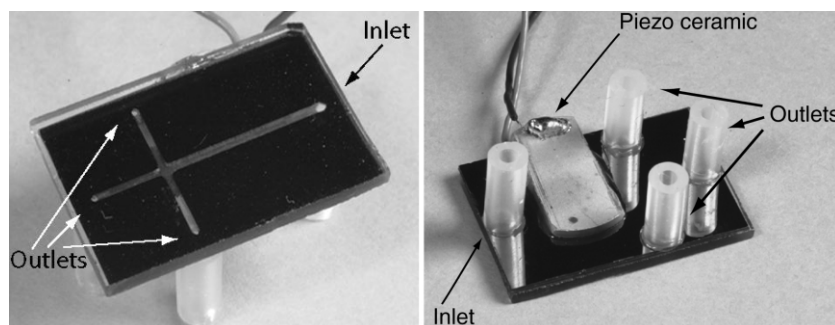


Fig. 3 Front and rear side of a cross-type separation chip.

to the percentage total solid fraction in the fluid collected at all three outlets ($A + B$), eqn. (5).

$$\text{Separation efficiency} = 100 \cdot B / (A + B) \quad (5)$$

where:

A = relative particle fraction of the fluid collected from the centre outlet

B = relative particle fraction of the fluid collected from the side outlets

4 Results and discussion

4.1 Actuation

A benefit of arranging the actuator in plane with the separation chip is the large contact surface area for the piezoceramic actuator enabling a good coupling of the acoustic energy into the silicon chip. In spite of the fact that the actuator provides the acoustic signal from the back/bottom of the chip, the standing wave is obtained in plane with the silicon chip and orthogonal to the flow channel (Fig. 4) enabling continuous flow separation of particles.

4.2 Band formation

When particles are exposed to an acoustic force they will gather in the nodes or anti-nodes of the standing wave. Because of the laminar conditions in a small flow channel, particles once gathered in a defined lateral position will stay there even after leaving the acoustic force field, forming long bands of particles in the channel. When operating the separation channel in its fundamental resonance mode ($\lambda/2$) a single band formation was observed in the middle of the channel. However, the acoustic forces in the fundamental resonance mode were too weak to generate a well-defined particle band in the centre of the channel. The chips were therefore operated and the performance was investigated at the first harmonic ($2 \cdot \lambda/2$), where two bands were seen (Fig. 5 left). The higher operating frequency provided an improved particle focusing force as reasoned above, eqn. (3). There is also the possibility to generate multiple bands (Fig. 5 centre and right) in the separation channel at even higher harmonics.

4.3 Particle separator designs

Two different separators were designed and fabricated in silicon. Initially a cross-type design with the side outlet channels perpendicular to the inlet channel was made (Fig. 6a). The structure was 250 μm deep and the width and length of the inlet channel was 750 μm and 13 mm respectively. The cross-type design however displayed problems with stagnant zones as the fluid turned around the 90° corner into the side channels. Any air bubble or debris that entered the system was easily caught in the stagnant zone and was very hard to remove without disturbing the on-going separation. To solve that problem a new chip was designed, with the side channels leaving the separation channel at a 45° angle (Fig. 6b). In an attempt to make the separation structure even shorter, the inlet channel length was also reduced to 9 mm.

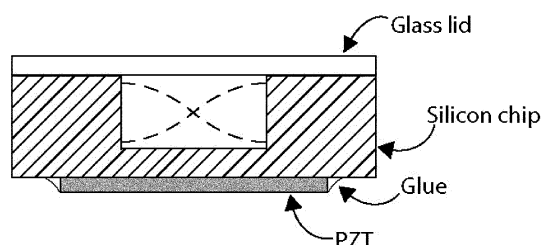


Fig. 4 A principal cross-section drawing of the assembled separation device, showing the separation channel with the piezoceramic element glued to the rear side of the microchip. The acoustic signal is tuned to fit the resonance criterion defined by the channel width, generating an acoustic standing wave (dashed) in plane with the silicon chip, orthogonal to the flow channel.

4.4 Results and discussion

The cross-type separator was operated in a two node mode ($2 \cdot \lambda/2$) with two bands and thus enriched particles were leaving *via* the side outlets as seen in Fig. 6. Studies of a varying operating voltage to the piezoceramic element (Fig. 7), at constant frequency of 1.956 MHz, constant flow of 0.3 ml min⁻¹ and constant blood phantom concentration of 10%, show, as expected, that a higher separation efficiency was achieved with increasing voltage.

To operate the piezoceramic element at voltages exceeding 22 volts at a flow of 0.3 ml min⁻¹ was not possible due to the fact that the high radiation forces trapped the particles in the ultrasonic field forming stationary particle clusters in the flow channel, which disturbed the laminar flow profile. High operating voltages will also cause an increase of temperature in the piezoceramic element, which may not exceed the Curie temperature of the ceramic since that will destroy the piezoelectric properties of the actuator.

The flow rate tests (Fig. 8) clearly show that lower flow rates provide a higher separation efficiency, which is the result of exposing the particles to the standing wave field for a longer time period, allowing more particles to reach their nodal position in the standing wave. The flow rate, voltage and the blood phantom concentration were maintained constant at 1.956 MHz, 15 V_{pp} (Voltage peak to peak) and 10% respectively. The voltage 15 V_{pp} was chosen since higher voltages in the lower flow rate range, below 0.1 ml min⁻¹, caused particle trapping/clustering and subsequent blocking of the flow channel.

Tests with different blood phantom concentrations (Fig. 9) showed, as expected, that the lower concentration yielded higher

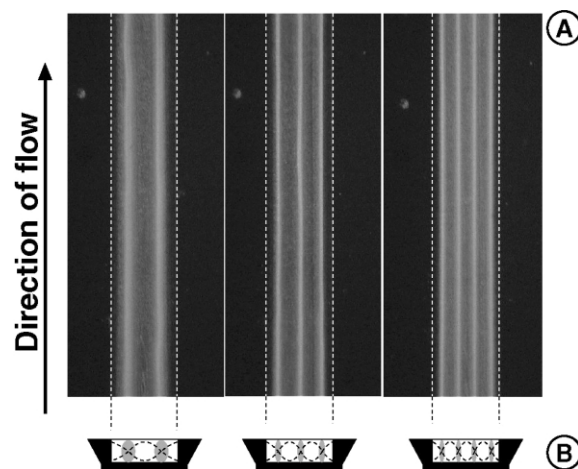


Fig. 5 Particle enrichment in the micro channel. The bands show the enriched particles in resonance mode, 1st, 2nd and 3rd harmonic with 2, 3 and 4 bands respectively, A) top view microscope photographs and B) principal separation channel cross-sections. Channel width: 750 μm , channel depth: 250 μm .

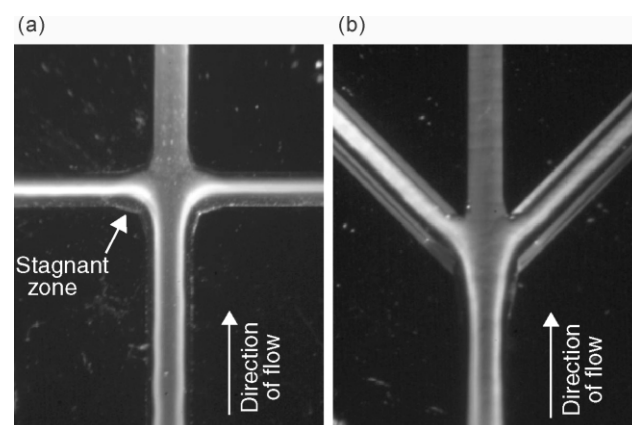


Fig. 6 a. Cross-type structure with a two band formation. b. 45°-structure with a two band formation.

separation efficiency. With increasing particle concentration, the side channels collecting the enriched particles will eventually be saturated, spilling over into the centre channel, which results in a decreased separation efficiency. As the blood phantom concentration increased, the separation efficiency decreased towards 67% (not shown), which would be the case when equal amounts of particles exit all outlets. This is also the case when no ultrasound is applied.

At its best, a separation efficiency of approximately 90% was achieved for the cross-type structure, *i.e.* almost 90% of the particles were collected through the side channels together with 2/3 of the fluid volume, at flow velocities less than 0.2 ml min^{-1} . The structure had however problems with stagnant zones as the fluid turned around the 90° corner. By changing the orientation of the side channels to 45° [Fig. 6b] the stagnant zones were reduced, and the separation process was improved.

Besides the change of the side channel angle for the 45° -structure, the inlet channel length was also shortened from 13 to 9 mm. In the investigation of the influence of the actuation voltage the 45° -structure showed approximately 10% higher separation efficiency at lower voltages (10 Vpp) as compared to the cross-structure; compare Fig. 7 and Fig. 10. At higher voltages both structures approached a separation efficiency close to 90%. It

should be noted that the 45° -structure outperforms the cross-structure in spite of the fact that the separation channel was 4 mm shorter than the cross-structure.

The shorter separation channel resulted in a reduced retention time in the acoustic force field and thus the time for the particles to be focused were reduced by approximately 30%. A comparison of the separation efficiency of the two chip designs regarding the influence of flow rate (Fig. 8 and Fig. 11) and concentration of blood phantom (Fig. 9 and Fig. 12) respectively also disclosed that the 45° -structure performs better than the cross-structure. Much of the improved performance for the 45° -structure is attributed to the better flow profiles, avoiding rapid changes of the flow directions. This was also visually confirmed while performing the experiments. Commonly the cross-structure displayed a loss of particles from the focused bands into the centre outlet as the two bands turned around the 90° corner to its outlets. This was not as clearly seen for the 45° -structure. Both separator types displayed a maximum separation ratio of about 90% at extreme operating parameters.

In order to further optimise the proposed acoustic separation technology it would be preferable to move forward with a theoretical model describing the microfluidic and particle separation efficiency properties of the micro chip. The current state of

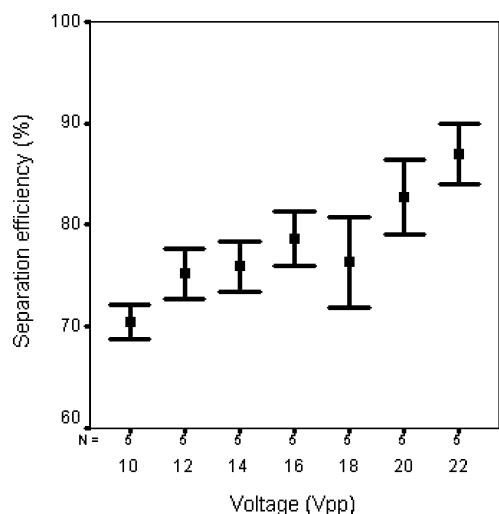


Fig. 7 Separation efficiency of a cross-type structure as a function of the excitation voltage to the piezoceramic element. Constant frequency of 1.956 MHz, a flow of 0.3 ml min^{-1} and 10% concentration of blood phantom were used.

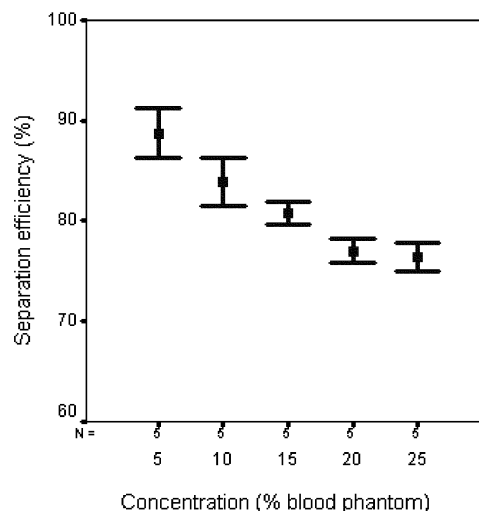


Fig. 9 Separation efficiency of a cross-type structure as a function of the concentration of the blood phantom. Constant frequency of 1.956 MHz, 20 Vpp and a flow of 0.3 ml min^{-1} .

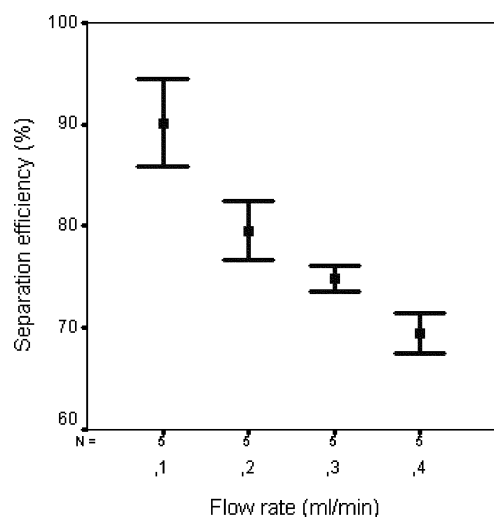


Fig. 8 Separation efficiency of a cross-type structure as a function of the flow. A constant frequency of 1.956 MHz, 15 Vpp, and 10% concentration of blood phantom was used.

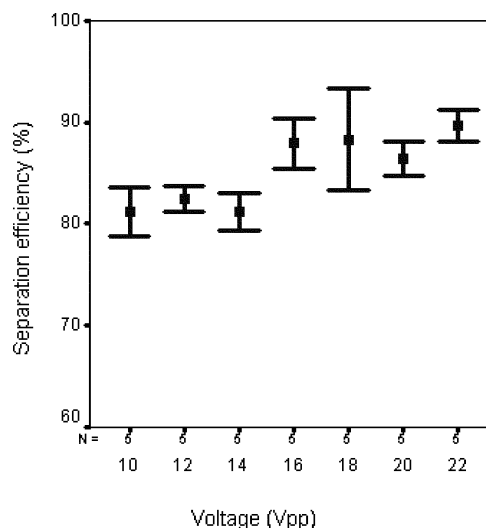


Fig. 10 Separation efficiency of a 45° -structure as a function of the excitation voltage to the piezoceramic element. A constant frequency of 1.970 MHz, a flow of 0.3 ml min^{-1} and 10% concentration of blood phantom was used.

modelling such a system still holds seemingly large deviations from experimental data. Hawkes and Coakley¹ have presented theoretical modelling of acoustic particle separation and compared these with experimental data demonstrating promising results. However, a further improvement of the model would be desired in order to predict the experimental outcome of a new separation device. Before a theoretical model actually would provide useful data in the work presented herein a much more detailed investigation of several physical parameters is needed, *e.g.* the acoustic field distribution in the separation channel is not easily derived as it is dependent on the coupling of the mechanical oscillation from the piezoceramic actuator to the separation channel *via* the bulk silicon. The wave propagation in the silicon chip and hence the obtained

acoustic interference pattern is a complex modelling task. The modelling of the fluidics does not pose a problem as the system is operated in an laminar flow regime, Reynolds number ≈ 20 . A further complication in defining a correct model is the fact that the fluid temporally undergoes a spatial reconfiguration with a change in physical properties, *e.g.* apparent density and viscosity (due to changing particle densities), while passing through the separation channel. Also, the effect of secondary forces on the particles, Bjerknes forces,^{10,11} pose a further complex addition to the total model needed as the mean interparticle distance is varying in the separation channel along the channel length.

5 Conclusions

This paper demonstrates successful on-line particle separation in silicon microchips using acoustic forces. Ultrasonic excitation of the micro fluidic channel, matching the ultrasound frequency to the channel width, enabled the focusing of particles to defined flow lines in the streaming fluid and thus the collection of a particle enriched fluid in the side channel outlets. 90% of the particles were recovered in 67% of the original volume. By increasing the frequency to higher resonance harmonics, controlled higher order particle band formation (3 and 4 bands) was demonstrated. The chip based separation approach will in future versions enable serial connection of separators for a sequential enrichment and at the end a net total higher particle enrichment factor than currently obtained. In order to improve the separation efficiency it would be desirable to confine the particles to a smaller zone. By reducing the channel width the particles are expected to be focused in a narrower band as the force on the particles increases with increasing frequency since a narrower channel has a higher resonance frequency.

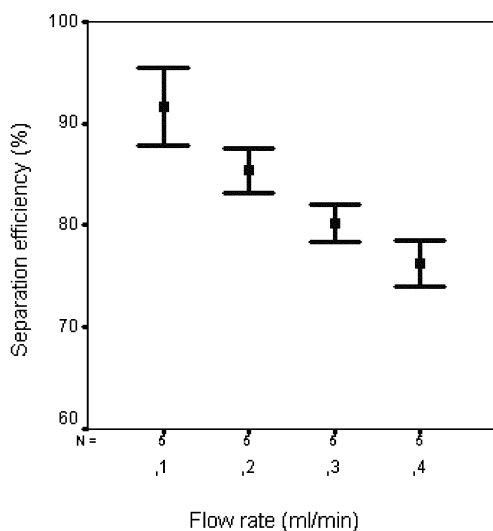


Fig. 11 Separation efficiency of a 45°-structure as a function of the flow rate. A constant frequency of 1.970 MHz, 15 Vpp and 10% concentration of blood phantom was used.

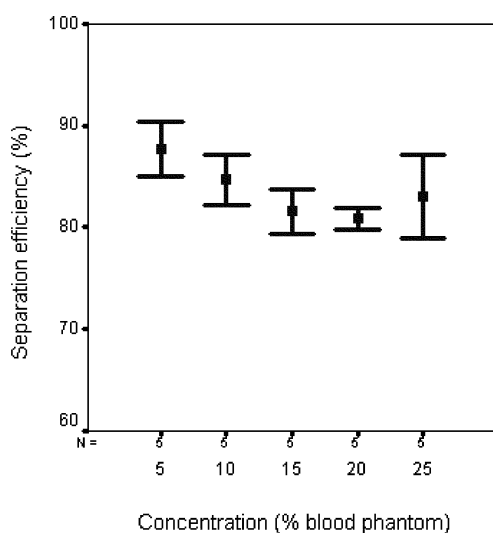


Fig. 12 Separation efficiency of a 45°-structure as a function of the concentration of the blood phantom. Constant frequency of 1.970 MHz, 20 Vpp and a flow of 0.3 ml min⁻¹.

References

- 1 J. J. Hawkes and W. T. Coakley, Force field particle filter, combining ultrasound standing waves and laminar flow, *Sens. Actuators B*, 2001, **75**, 213–222.
- 2 M. Gröschl, Ultrasonic separation of suspended particles – Part I: Fundamentals, *Acust. Acta Acust.*, 1998, **84**, 432–447.
- 3 M. Gröschl, Ultrasonic separation of suspended particles – Part II: Design and operation of separation devices, *Acust. Acta Acust.*, 1998, **84**, 632–642.
- 4 T. L. Tolt and D. L. Feke, Separation of dispersed phases from liquids in acoustically driven chambers, *Chem. Eng. Sci.*, 1993, **48**, 527–540.
- 5 D. A. Johnson and D. L. Feke, Methodology for fractionating suspended particles using ultrasonic standing wave and divided flow fields, *Sep. Technol.*, 1995, **5**, 251–258.
- 6 K. Yasuda, S. Umemura and K. Takeda, Studies on particle separation by acoustic radiation force and electrostatic force, *Jpn. J. Appl. Phys.*, 1996, **1**, 3295–3299.
- 7 K. Yasuda, S. Umemura and K. Takeda, Concentration and fractionation of small particles in liquid by ultrasound, *Jpn. J. Appl. Phys.*, 1995, **1**, 2715–2720.
- 8 J. J. Hawkes, W. T. Coakley, M. Gröschl, E. Benes, S. Armstrong, P. J. Tasker and H. Nowotny, Single half-wavelength ultrasonic particle filter: Predictions of the transfer matrix multilayer resonator model and experimental filtration results, *J. Acoust. Soc. Am.*, 2002, **111**.
- 9 K. Yosioka and Y. Kawasima, Acoustic radiation pressure on a compressible sphere, *Acustica*, 1955, **5**, 167–173.
- 10 L. A. Crum, Bjerknes forces on bubbles in a stationary sound field, *J. Acoust. Soc. Am.*, 1975, **57**(6), 1363–1370.
- 11 M. A. H. Weiser and R. E. Apfel, Interparticle forces on red cells in a standing wave field, *Acustica*, 1984, **56**, 114–119.